Characterizing and monitoring respiratory aerosols by light scattering

Yong-Le Pan, Kevin B. Aptowicz, and Richard K. Chang

Department of Applied Physics and Center for Laser Diagnostics, Yale University, New Haven, Connecticut 06520

Matt Hart and Jay D. Eversole

U.S. Naval Research Laboratory, Code 5611, 4555 Overlook Avenue S.W., Washington, D.C. 20375

The elastic-scattering intensity pattern from a single particle as a function of spherical coordinate angles θ and ϕ provides detailed information on the pattern's morphology. By use of an ellipsoidal reflector and a CCD camera, a single-laser-shot intensity pattern from a large angular range (θ from 90° to 168° and ϕ from 0° to 360°) was detected from a single aerosol (e.g., a *Bacillus subtilis* spore, a 1-μm-diameter polystyrene latex sphere, or a cluster of either of these) flowing through the reflector's focal volume at 5 m/s. Noticeable differences in the large-angle-range two-dimensional angular optical scattering (LATAOS) suggest that the LATAOS pattern could be useful in differentiating and classifying life-threatening aerosols from normal background aerosols. © 2003 Optical Society of America

OCIS codes: 000.1430, 010.1100, 290.5820, 290.5850.

Protection from threats of bioterrorism by dispersal of pathogenic aerosols requires advanced detection systems. It is highly desirable to be able to detect and distinguish *in situ,* continually, and in real time, potentially life-threatening bioaerosols from normal background conditions, especially in the respirable size range of 1−10-μm diameter.[1,2] Currently proposed sensors for such detection are based on laser-induced fluorescence[3,4]; mass spectrometry[5]; microchip-based mass, capacitance, and calorimetric transducers[6]; lidar[7]; and elastic light scattering.[8−14] Among these processes, elastic scattering is the most sensitive technique and has potential for providing size, shape, and surface-texture information on individual particles.

Extracting information about aerosols by elastic scattering started as early as the 17th century when Descartes and others explained the rainbow.[15−17] In the past century, most research in this area was devoted to the development of computational methods, such as Lorenz−Mie theory,[18] and to one-dimensional angular scattering measurements (see, e.g., Refs. 8 and 9). Such one-dimensional data can hardly supply adequate information with which to characterize nonspherical aerosols with random orientations. Recently attention has necessarily shifted toward natural aerosols,[10−12,14] and controlled particles such as clusters of multispheres[14] that model aerosols found in the environment (e.g., pollens, soot aggregates, paper and wood fibers, sand, and animal dander).

The elastic-scattering distribution in the near-forward direction is dominated by diffraction and provides information about particle size and shape, whereas in the near-backward direction it is affected by more subtle particle characteristics such as surface texture, homogeneity, and refractive index. Thus, potentially useful information is contained in the scattered intensity, $I(\theta, \phi)$,[10−14] where polar angle θ relative to the z axis is defined by the incident laser beam and azimuthal angle ϕ relative to the x axis is defined as perpendicular to the laboratory floor.

Many elastic-scattering-based commercial instruments, such as DAWN,[10] are available to provide size or shape information on ambient aerosols and to measure discrete scattered-light intensities at preset angles with multiple detectors. Spatial intensity distributions have also been extensively investigated for fibers and other nonspherical particles by use of specially shaped detector array chips as well as CCD cameras.[11,12] However, we are aware of few investigations of individual flowing bioaerosols with elastic scattering transformed to $I(\theta, \phi)$. $I(\theta, \phi)$ for some prolate-oblate-shaped liquid droplets and clusters of polystyrene latex (PSL) spheres or *Bacillus subtilis* var. niger (BG) spores within a limited range ($\theta = \pm 3.5°$ and $\phi = \pm 14°$) were described in Ref. 14.

We describe here a significant advancement of the elastic-scattering technique that uses an ellipsoidal reflector to collect essentially the entire backscattering over a subtended solid angle greater than 2π sr. The scattered light that results from one laser shot (70 ns) on an individual flowing particle is detected by an image-intensified CCD (ICCD) camera. By use of a Q-switched laser instead of a cw laser the individual flowing aerosols are spatially frozen, resulting in higher-quality scattering patterns. Particles exiting from a specially designed nozzle are moving in a straight line at approximately 5 m/s. Scattered patterns are recorded for θ from nearly 180° to 90° (back hemisphere) or from nearly 0° to 90° (front hemisphere) and for an entire 360° of ϕ. Such large-angle-range two-dimensional angular optical scattering (LATAOS) data are crucial for those who attempt the inversion procedure of reconstructing the aerosol morphology from scattering distribution.

A simplified schematic of the experimental arrangement is shown in Fig. 1(a). The key components of the system are as follows: (1) an aerosol generator; (2) a cw diode laser (635 nm) and photomultiplier tube (PMT) to detect the scattering associated with the random arrival of aerosols just above the focal point of
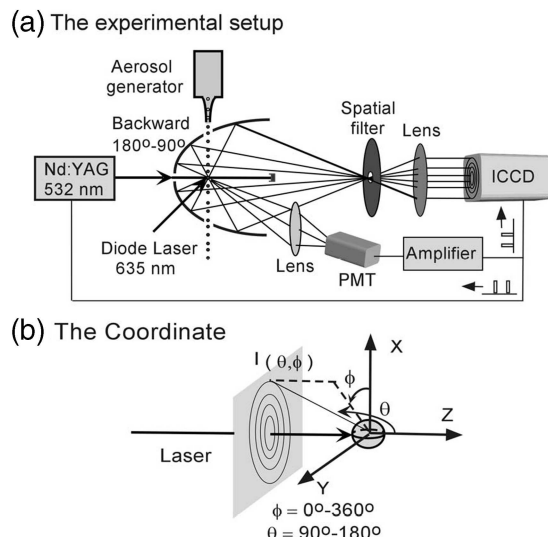
Fig. 1. Experimental setup for LATAOS measurement and corresponding coordinates.

the ellipsoidal reflector and to trigger the illuminating laser and the ICCD camera; (3) a Q-switched laser (532 nm) to illuminate the aerosols; (4) an ellipsoidal reflector to collect the scattered light; (5) a camera lens (f-number, 1.2; $f = 55$ mm) to project the scattered light to a plane; and (6) an ICCD camera to record the scattering pattern.

Either of two aerosol generators was used, depending on the type of aerosol being examined. First, a flow-cytometry reservoir–nozzle system was used to produce spheroidal water or ethanol droplets.[19] Second, an ink-jet aerosol generator[20] was used to produce single dry BG spores,[21] PSL spheres, riboflavin particles, and clusters of a specific size of either BG spores or PSL spheres. Samples of the dry particles were collected for subsequence characterization with scanning electron microscopy (SEM).

The ellipsoidal reflector is used to maximize the solid angle of the scattered light that is being detected [see the coordinate system in Fig. 1(b)]. It reflects the scattered light over the range $\theta = 48°-164°$, $\phi = 0°-360°$ (covering 63% of 4π sr) to the second focal point. The laser entrance hole prevents collection at $\theta = 164°-180°$. The iris at the second focal point, in combination with a beam block, allows only the reflected rays to pass but blocks both forward-scattered light and the direct laser beam. The camera-recorded image $I(x, y)$ was transformed into the angular scattered pattern $I(\theta, \phi)$ by a ray tracing technique.

Figure 2 shows typical backward hemisphere LATAOS patterns from a single 1-μm-diameter PSL sphere and from a single BG spore (anthrax simulant, sausagelike, ~ 1 μm in length, 0.5 μm in diameter; see the SEM images at the bottom right). The surface of a spherical PSL particle is smooth, whereas that of a BG spore is rough. Furthermore, the PSL sphere is homogeneous, with a refractive index near 1.6, whereas the BG spore has an inhomogeneous refractive-index structure (the mean value is

~ 1.5).[22] These physical differences are manifested in the distinctive backscattered patterns depicted.

There are certain features of the patterns that are artifacts of experimental components. The dark circle in the center and the horizontal black line on the right semicircle (Fig. 2) are caused by the beam dump and its mount, respectively. The four black semicircles, at the top, bottom, left, and right, are the result of holes located at $\theta = 90°$ in the reflector for aerosols and diode laser to pass through.

The LATAOS pattern from a 1-μm PSL sphere shows the well-known ring structure expected from Mie theory. By contrast, the pattern from a single BG spore is far less symmetrical, with islandlike features. The patterns from different individual BG spores are not identical to one another because (1) the different BG spores, carried by the gas flow, are at random orientations related to the illuminating beam and (2) the surface irregularity of BG spores varies from one to another, but all patterns are composed of intensity islands with similar sizes and shapes.

Droplets with or without inclusions are some of the most common environmental aerosols. LATAOS patterns from several nonspherical particles, such as water and ethanol spheroidal droplets and needlelike riboflavin particles, were examined. Figures 3(a)–3(c) show LATAOS patterns from alcohol droplets with fixed volume and aspect ratios that vary from 0.87 to 1.11. The symmetry axis of these droplets is horizontal, nearly perpendicular to the polarization of the incident laser. Shape-defining features are seen in the patterns as the shapes of the droplets vary from oblate to prolate. The insets are video images of the illuminated droplets. Figure 3(d) shows a typical LATAOS pattern from a single riboflavin particle. SEM images of dried riboflavin appear as needlelike crystalline structures. Their patterns resemble the diffraction of a fiber and show the projected tilt angle relative to the illuminating laser.

One of the main emphases of this research is to find ways to use LATAOS to classify respirable aerosols, especially clusters, within 1−10 μm. Therefore LATAOS from different-sized clusters composed of different-sized and -shaped primary particles was studied. Figure 4 shows typical LATAOS patterns
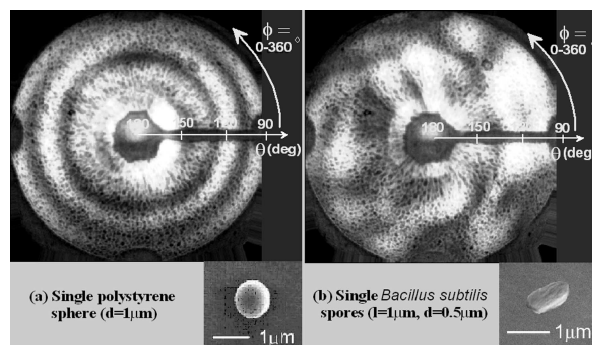
Fig. 2. Typical backward hemisphere LATAOS patterns from (a) a single 1-μm-diameter PSL sphere and (b) a single BG vegetative spore. A typical SEM image of each type of particle is also shown.
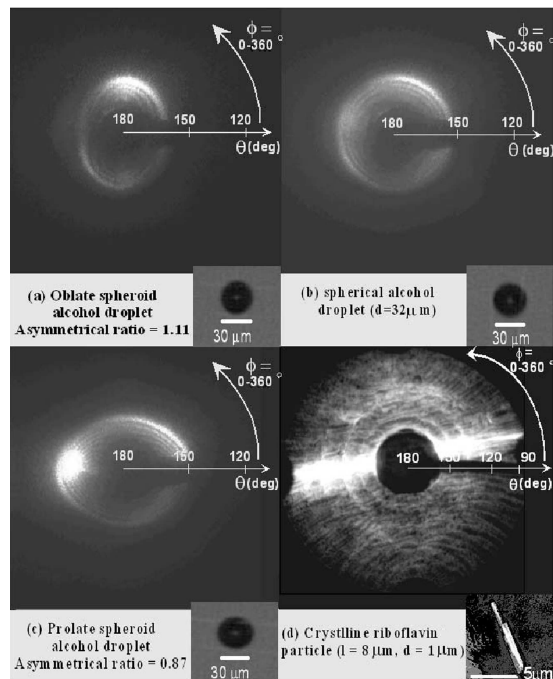
Fig. 3. Typical backward hemisphere LATAOS patterns from alcohol droplets (with volume equal to that of a 32-μm-diameter sphere) with aspect ratios that vary from (a) 1.11 (oblate), (b) 1.00 (sphere), and (c) 0.87 (prolate) as well as from (d) a single, needlelike riboflavin particle, ~ 8 μm in length.
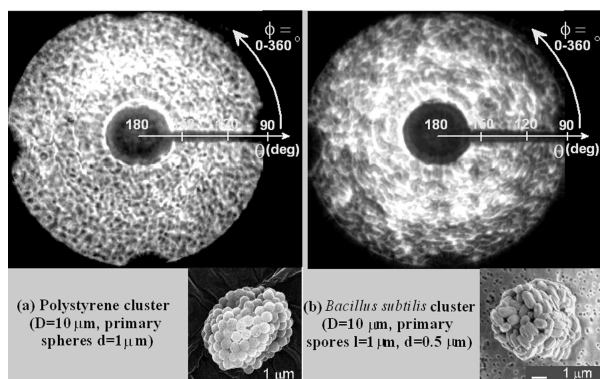
Fig. 4. Typical backward hemispherical LATAOS patterns from (a) a 10-μm cluster formed from 1-μm PSL spheres and (b) a 10-μm cluster formed from BG vegetative spores. Typical SEM images of the PSL and BG clusters are shown.

from two clusters, both with an approximate diameter of 10 μm. Figures 4(a) and 4(b) show clusters consisting of 1-μm PSL spheres and BG spores, respectively (see the SEM images at the bottom right). The two LATAOS patterns of clusters formed by PSL spheres and BG spores can be readily distinguished by eye. Therefore, by fast computer image processing, suspect life-threatening aerosols can be detected, *in situ* and in real time, by their characteristic LATAOS patterns and differentiated from other background aerosols.

References

1. D. A. Henderson, Science **283,** 1279 (1999).
2. L. A. Vanderberg, Appl. Spectrosc. **54,** 376a (2000).
3. Y. L. Pan, S. Holler, R. K. Chang, S. C. Hill, R. G. Pinnick, S. Niles, and J. R. Bottiger, Opt. Lett. **24,** 116 (1999).
4. J. D. Eversole, J. J. Hardgrove, W. K. Cary, Jr., D. P. Choulas, and M. Seaver, Field Anal. Chem. Tech. **3,** 249 (1999).
5. T. Peter, Science **273,** 1352 (1996).
6. C. Hagleiter, A. Hierlemann, D. Lange, A. Kummer, N. Kerness, O. Brand, and H. Baltes, Nature **414,** 293 (2001).
7. A. Thomasson, S. Geffroy, E. Frejafon, D. Weidauer, R. Fabian, Y. Godet, M. Nomine, T. Menard, P. Rairoux, D. Moeller, and J. P. Wolf, Appl. Phys. B **74,** 453 (2002).
8. P. J. Wyatt, Nature **221,** 1257 (1969).
9. M. Bartholdi, G. C. Salzman, R. D. Hiebert, and M. Kerker, Appl. Opt. **10,** 1573 (1980).
10. P. J. Wyatt, K. L. Schehrer, S. D. Phillips, C. Jackson, Y. J. Chang, R. G. Parker, D. T. Phillips, and J. R. Bottiger, Appl. Opt. **27,** 217 (1988).
11. P. H. Kaye, E. Hirst, J. M. Clark, and F. Micheli, J. Aerosol Sci. **23,** 597 (1992).
12. P. H. Kaye, K. Alexander-Buckley, E. Hirst, and S. Sauders, J. Geophys. Res. D **14,** 19215 (1996).
13. M. D. Barnes, N. Lermer, W. B. Whitten, and J. M. Ramsey, Rev. Sci. Instrum. **68,** 2287 (1997).
14. S. Holler, Y. L. Pan, R. K. Chang, J. R. Bottiger, S. C. Hill, and D. B. Hillis, Opt. Lett. **23,** 1489 (1998).
15. Rene Descartes, *Discours de la Méthode pour Bien Conduire Sa Raison et Chercher la Vérité dans les Sciences* (La Dioptrique, Paris, 1637), 2nd appendix.
16. J. A. Adam, Phys. Rep. Phys. Lett. **356,** 229 (2002).
17. D. S. Langley and P. L. Marston, Appl. Opt. **37,** 1520 (1998).
18. M. I. Mishchenko, L. D. Travis, and D. W. Mackowshi, J. Quant. Spectrosc. Radiat. Transfer **55,** 535 (1996).
19. Cytomation, Inc., 4850 Innovation Drive, Fort Collins, Colo. 80525.
20. J. R. Bottiger, P. J. Deluca, E. W. Stuebing, and D. R. Vanreenaen, J. Aerosol Sci. **29,** S965 (1998).
21. *Bacillus subtilis* var. niger spores (BG) supplied by Edgewood Chemical Biological Center, Aberdeen Proving Grounds, Md.
22. P. J. Wyatt, Appl. Opt. **7,** 1879 (1968).